Engineering Journal of Qatar University, Vol. 3, 1990.

"AN IMPROVED MODEL DESCRIBING MASS TRANSFER IN THREE-PHASE FLUIDIZED BEDS"

By

Abdul-Fattah A. Asfour
Chemical Engineering Department
Faculty of Engineering, Qatar University
Doha, Qatar - Arabian Gulf

ABSTRACT

A model for describing mass fransfer in three-phase fluidized beds has been developed and tested using experimental data.

The presence of two distinguishable mass transfer zones in three-phase fluidized beds led to the idea of interfacing a plug flow model (PFM) with an axial dispersion model (ADM) at the separation boundary between these zones to yield the proposed model.

The model reported here has been valildated at a wide range of operating conditions and proved to perform better than other existing models.

1. INTRODUCTION

Models describing mass transfer in three-phase fluidized beds have become a subject that is currently a lot of interest. Several models have been suggeste in the literature and are being employed for the calculation of volumetric mass transfer coefficients.

Most of the studies of mass transfer in three-phase fluidized beds adopted the axial dispersion model (ADM) or the plug flow model (PFM), i.e. Ostergaard and Suchozebriski (1986), Ostergaard and Fosbol (1972), Lee and Worthington

(1974) , Dhanuka and Stepank (1980), Cherry et al. (1978). Other investigators, e.g., Decker et al. (1974 and 1983) and Alvarez-Cuenca et al. (1979) reported experimental tests for the validity of such models.

Alvarez-Cuenca (1979) and Alvarez-Cuenca et al. (1984) utilized the system water-oxygen-glass beads in their three-phase fluidization studies and reported the existence of two clearly distinguishable mass transfer zones in three-phase fluidized beds. The first zone is near the distributor and is termed the "grid zone". In this zone plug flow conditions prevail and a great deal of mass of transfer (oxygenation) takes place. The second zone is termed the "bulk zone". Relatively much less mass transfer (oxygenation) takes place in such a zone. Consequently, some backmixing, or probably dispersed plug flow, is more dominant in this zone. Alvarez-Cuenca (1979) suggested utilizing concentration contour diagrams (similar to those shown in Figures 1 and 2) for identifying the different mass transfer zones.

The existence of two mass transfer zones led Alvarez-Cuenca (1979) to develop a two-zone model (T-ZM), which according to him, represented a significant improvement over the axial dispersion and plug fow models. The two-zone model results from interfacing two plug models at the boundary of separation between results the two mass transfer zones.

Deckwer et al. (1983) have analyzed, from a experimental standpoint, the validity of the axial dispersion model and the two-zone model. Unfortunately, we cannot accept their arguement concerning the T-ZM, since they deliverately ignored in their analysis, the experimental data obtained in the region lying in the immediate vicinity of the distributor where a great deal of oxygenation takes place.

The existence of two easily distinguishable mass transfer zone in three-phase fluidized beds was obrserved in our study. Therefore, it is difficult to believe that one model, i.e., PFM or ADM can describe mass transfer in such situations. This is because different conditions prevail in each zone. Therefore, the application of either the PFM or the ADM is tantamount to assuming that plug flow or axial dispersion conditions prevail in the column, which contrary to reality.

The main problem with the ADM is its constant axial dispersion coefficient. To overcome this problem an attempt was made to develop a "modified" ADM with a variable coefficient. However, the final form of the model obtained was cumbersome and difficult to use, even when for simplicity it was assumed that the change in the axial dispersion coefficient was linear. Consequently, such an approarch was discarded.

Alvarez-Cuenca's development of the T-ZM by interfacing two plug flow models at the separation boundary between the two mass transfer zone does not, in reality, solve the problem since it assumes that plug flow conditions prevail in each zone. Consequently, the T-ZM lacks a great deal from the physical significance standpoint.

The T-ZM gave better fit to the expirement data, as reported by Alvarez-Cuenca (1979), than the PFM. This can probably be attributed to the fact that it contains two adjustable parameters whereas the PFM has only one adjustable parameter. On the other hand, it gives better fit than the ADM since it contains only one exponential term versus two in case of the ADM. The exponential terms, if not treated properly and if a proper initial guess is not made, may lead to errouneous results. Therefore, the main advantage of the T-ZM over the ADM is that it is much easier to use.

The existence of the two distinct mass transfer zones led to the idea of interfacing a PFM and an ADM at the separation boundary. This resulted in a better and more physically meaningful model than the aforementioned models.

Consequently, the objective of this study is to present the development of such a model and to validate the model using experimental data. The derivation of the model is given in Appendix A.

Recognize, however, that the proposed model contains more parameters than any of the aforementioned models. Whereas some may consider this a disadvantage, we can counter argue that such a disdvantage is outweighed by the fact that such a model describes mass transfer in three-phase fluidized beds more accurately than any other model. In addition it is developed on more realistic grounds with proper physical meaning.

Alvarez-Cuenca (1979) and Alvarez-Cuenca et al. (1984) showed that the T-ZM conforms more closely to experimental data than either the PFM or the ADM. Therefore, we will restrict ourselves in this paper to comparing our proposed model with the T-ZM. We will utilize some of the experimental data reported by Alvarez-Cuenca (1979) as well as data generated in our laboratory in order to test our model at a wide range of operating conditions.

The parameters M, μ and θ given by Equations (A.4), (A.9) and (A.8) are determined from Equations (A.3, A.11, A.14 and A.15) by nonlinear regression (computer library subroutine ZXSSQ was used). Once the values of these parameters are obtained, Equations (A.8, A.9 and A.10) can be solved simultaneously to obtain the values of $(K_La)_B$ and E_y. Equation (A.4) is used to calculate $(K_L\ a)_G$.

The separation boundary parameter, b, depends on the liquid and gas superficial velocities as well as on the solid phase particle diameter. To provide a reliable correlation between b and the aforementioned variables, a large data base is required. We have just started an experimental program aimed at obtaining such a data base.

2. EXPERIMENTAL

The design of the experimental set-up used in this investigation is similar to that reported by Alvarez-Cuenca (1979), except that we provided 110 strategically located sampling ports in the two dimensional column in order to obtain more data points in the grid zone than those obtained by Alvarez-Cuenca (1979). A two dimensional column is a column in which two dimensions, viz. height and width are much larger than the third dimension, viz. depth. In the case reported in this study the height was about 200 cm., the 66 cm. and the depth 2.54 cm. The details of the experimental set-up are documented elsewhere (Nhaesi, 1986).

In order to test the two-zone model and the proposed model, it is important to employ different flow conditions. The liquid and gas superfecial velocity ranges employed were 5-12 cm/s and 8-43 cm/s, respectively. The solid phase (glass beads) used in this study consisted of monosized beads of 0.3 and 0.5 cm diameter. The tolerance was ±5% on the diameter and there was less than 1% irregularly shaped particles.

3. RESULTS AND DISCUSSION

The results of this study will be discussed under two sections. The first section is devoted to the experimental concentration profiles and contour diagrams. The second section is concerned with the proposed model; its analysis and comparison with the two-zone model. The volumetric mass transfer coefficient and the dispersion coefficient, Ey, are reported and the manner in which they vary with the gas and liquid superficial velocities is analyzed.

3.1 Concentration on Profiles:

The design of the two-dimensional column permits gathering oxygen concentration data from 110 strategically located sampling ports. The collected data are used to draw concentration profiles and in the preparation of pertinent contour diagrams. The oxygen concentration data along the center of the column were used to test the validity of the mathematical models which have been employed in this study.

The contour diagrams obtained in this study confirmed the existence of two clearly distinguishable mass transfer zones in three-phase fluidized beds as was reported earlier by Alvarez-Cuenca (1979). These two zones are usually separated by narrow transition area, which is termed the "boundary of separation."

In three-phase fluidized beds the separation boundary can be visually determined by use of contour diagrams. Such a boundary usually appears more or less parallel to the X-axis separating a series of concave and convex isograms (cf. Figure 1).

In other cases, the transition line is not readily distinguishable. In such situations the grid zone is characterized by higher isogram density than the bulk zone. The concentrated isograms in the grid zone are, abviously, a direct consequence of the high concentration gradients in this region. Such a case is

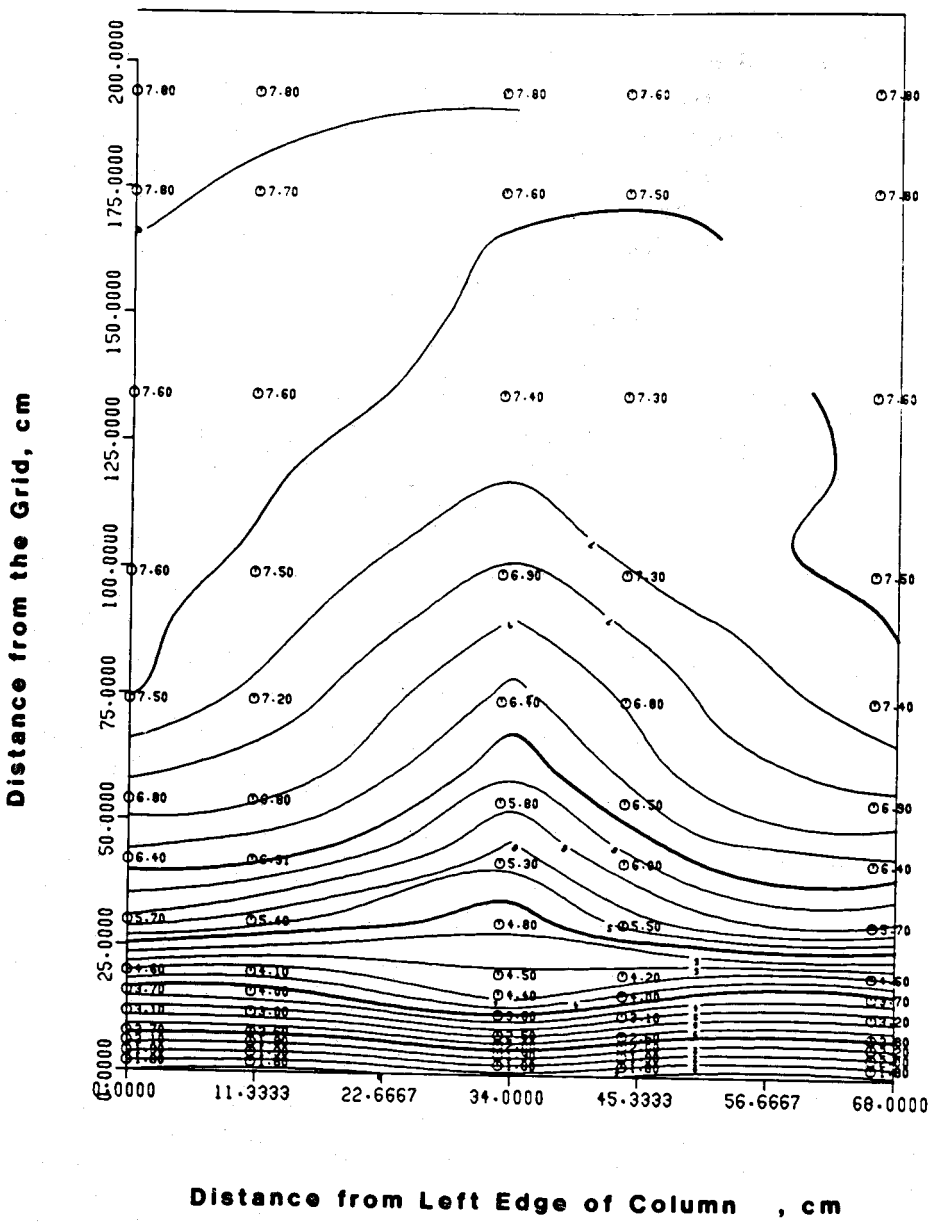

Figure 1 : Contour Diagram, D_p = 0.3 cm, V_g = 26 cm/s, and V_l = 12 cm/s.

depicted in Figure 2. Consequently, the separation boundary can be determined by determining the area in which there is the isogram density.

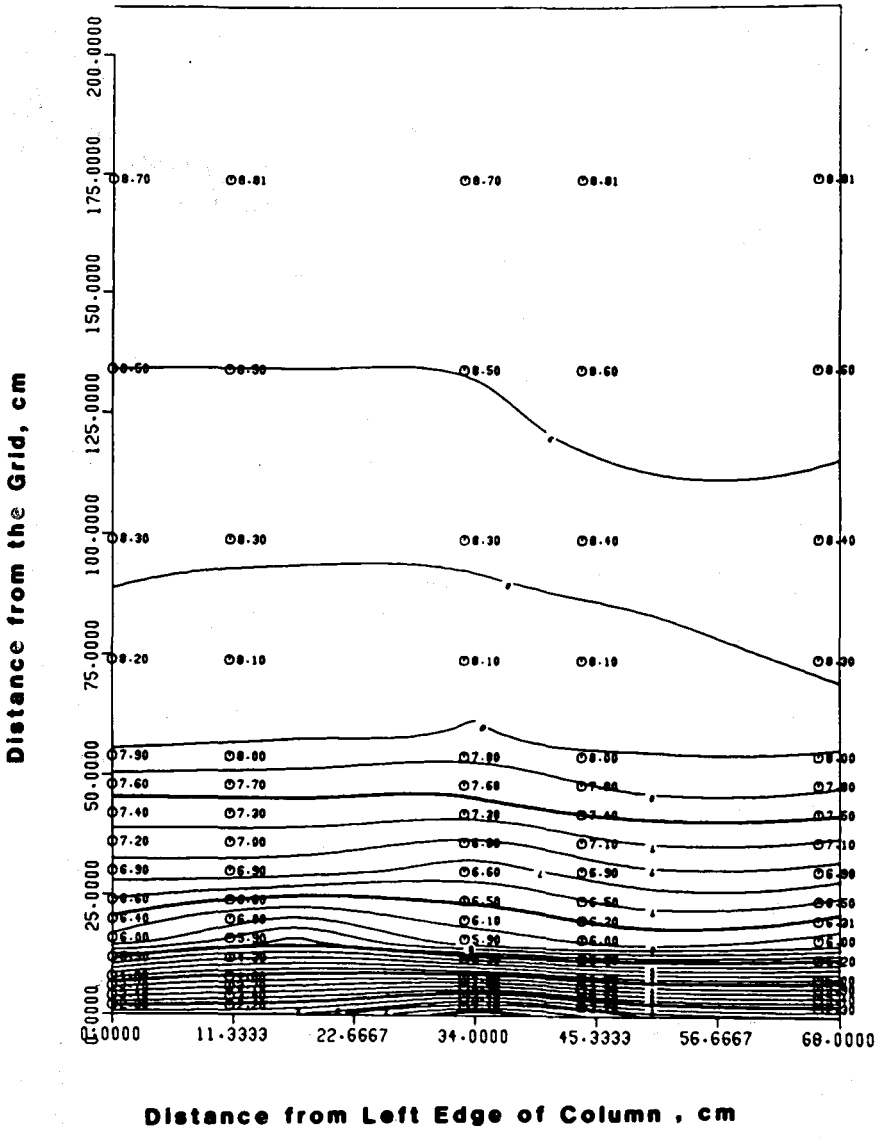

Figure 2 : Contour Diagram, D_p = 0.0 cm, V_g = 8cm/s, and V_1 = 5 cm/s.

In this study the separation boundary was found to vary from 20 to 60 cm above the grid. This variation results from changing the gas and liquid superficial velocities. In general, the demarcation between the two sections gets closer to the distributor as the gas and liquid superficial velocities increase (cf. Figures 3 and 4). Consequently, the oxygenation rate would increase and saturation is achieved at shorter distances from the grid. However, the data obtained in this study are not sufficient to indicate whether there is a dependence of the separation boundary parameter, b, on solid phase particle diameter. Investigating such an effect is currently underway.

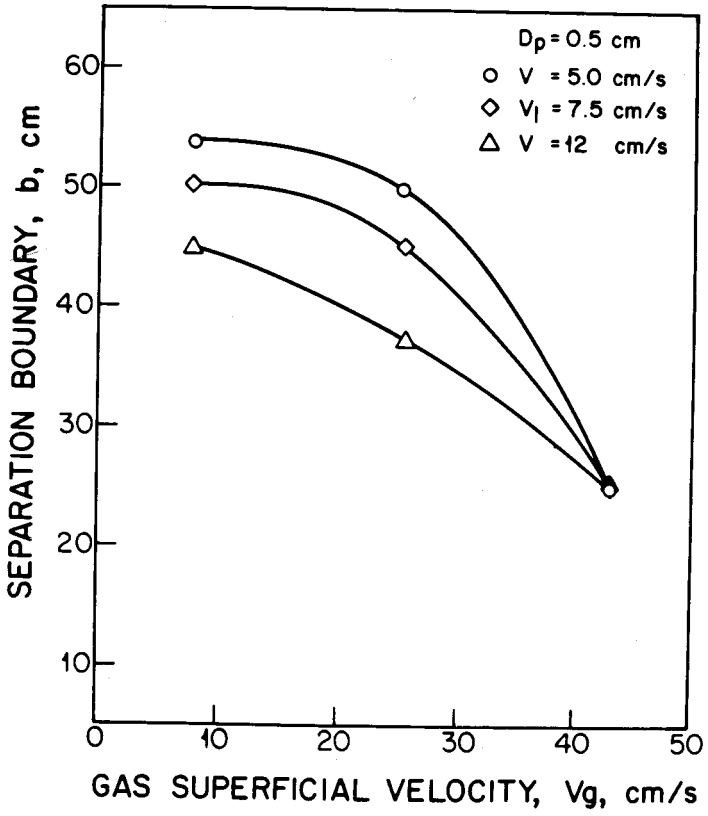

Figure 3 : Variation of the Separation Boundary Parameter, b, with the Superficial Fluid Velocities at D = 0.5 cm.

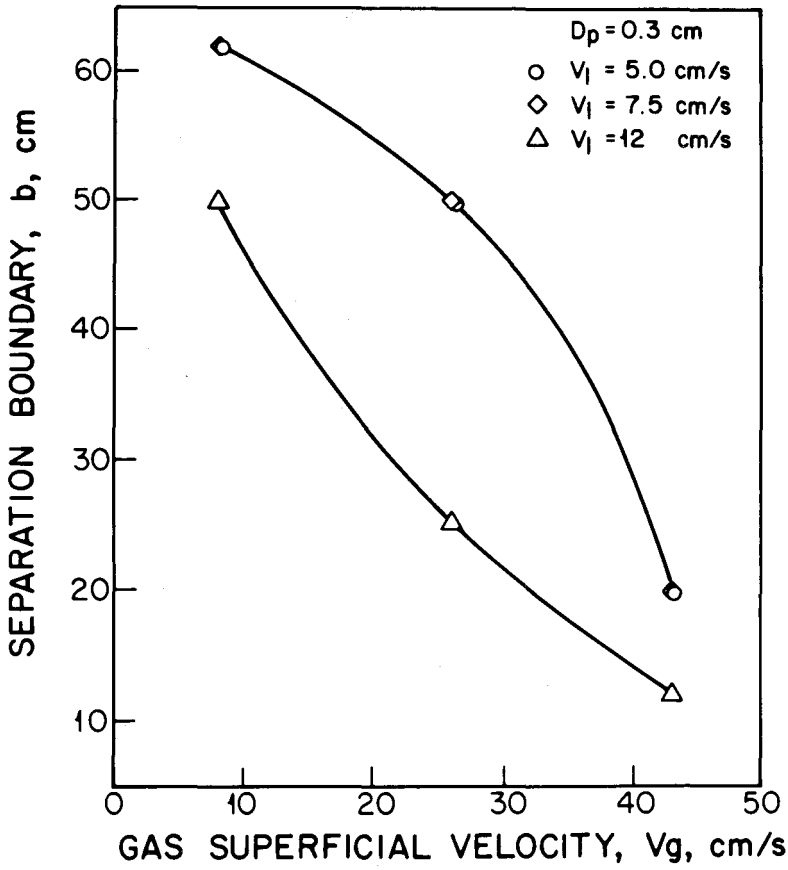

Figure 4 : Variation of the Separation Boundary Parameter, b, with the Superficial Fluid Velocities at D = 0.3 cm.

To establish a certain value for the separation boundary, the two zone model and the proposed model were solved for different values of b = y, namely, y = 36, 42 and 54 cm. The best fit to the experimental data was obtained at b = 36 cm. It should be pointed out that only discrete values of y are know (the sampling ports), therefore, when the concentration of oxygen at y = 36 cm was not measured, b is assumed to be 42 cm.

Typical concentration profiles in three-phase fluidized beds are depicted in Figure 5. At high gas superficial velocities (V_g = 43 cm/s) a steep rise in oxygen

concentrations occurs in the grid region. This rise corresponds to high concentration gradients. However, at a distance of about 20 cm from the grid, the rate of concentration increase starts to slow down until it reaches steady values close to top of the column. In this zone, the bulk zone, the concentration gradients are small due to backmixing. Also, the liquid phase approaches its saturation limit.

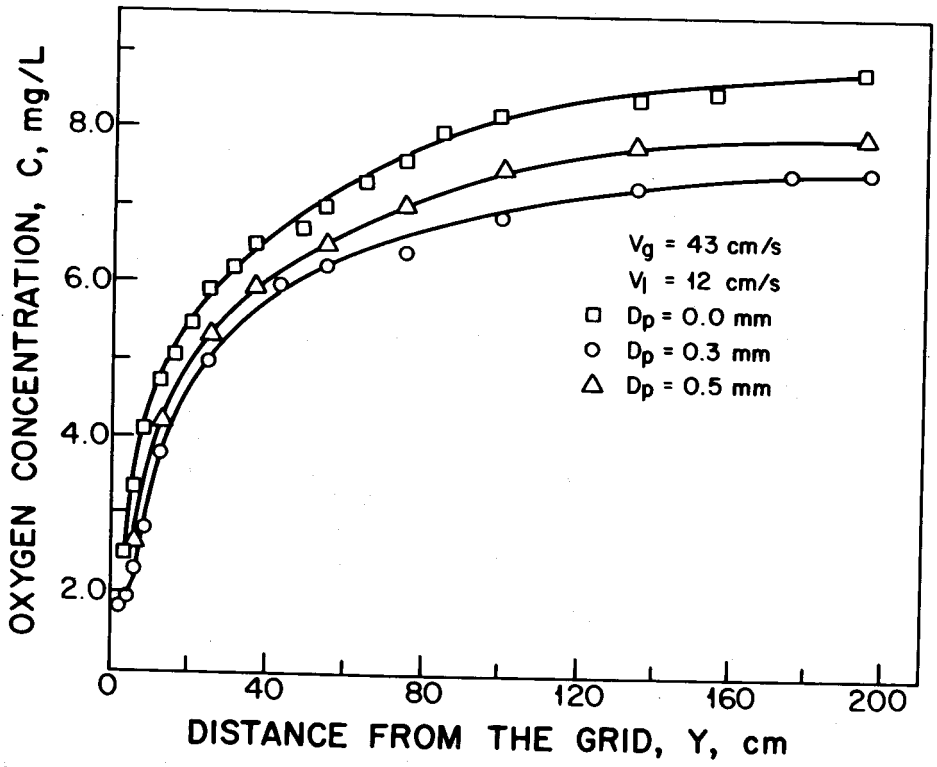

Figure 5 : Variation of the Experimental Oxygen Concentration with Solid-Phase Particle-Size at High Flow Rate.

At low gas superficial velocities, e.g. at V_g = 8 cm/s and 4 cm/s, the concentration profiles are generally S-shaped. These profiles are depicted in Figures 6, 7, and 8, respectively. It appears that the concentration remains almost constant in the grid region, then it increases gradually until it reaches a steady value.

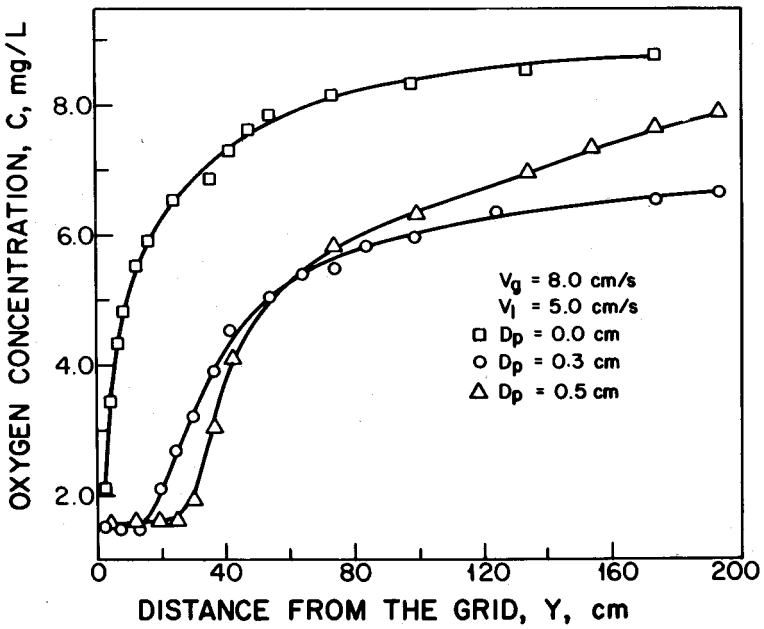

Figure 6 : Variation of the Experimental Oxygen Concentration with Solid-Phase Particle-Size at Low Flow Rate.

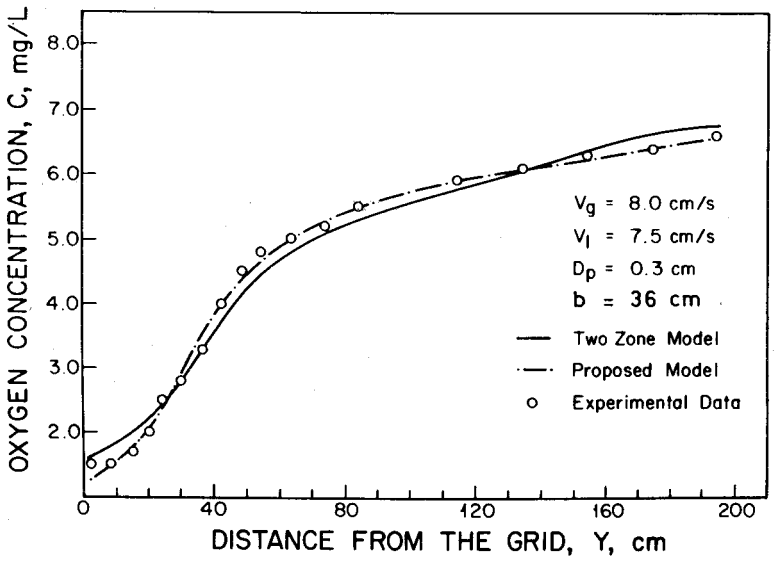

Figure 7 : Experimental and Predicted Oxygen Concentration.

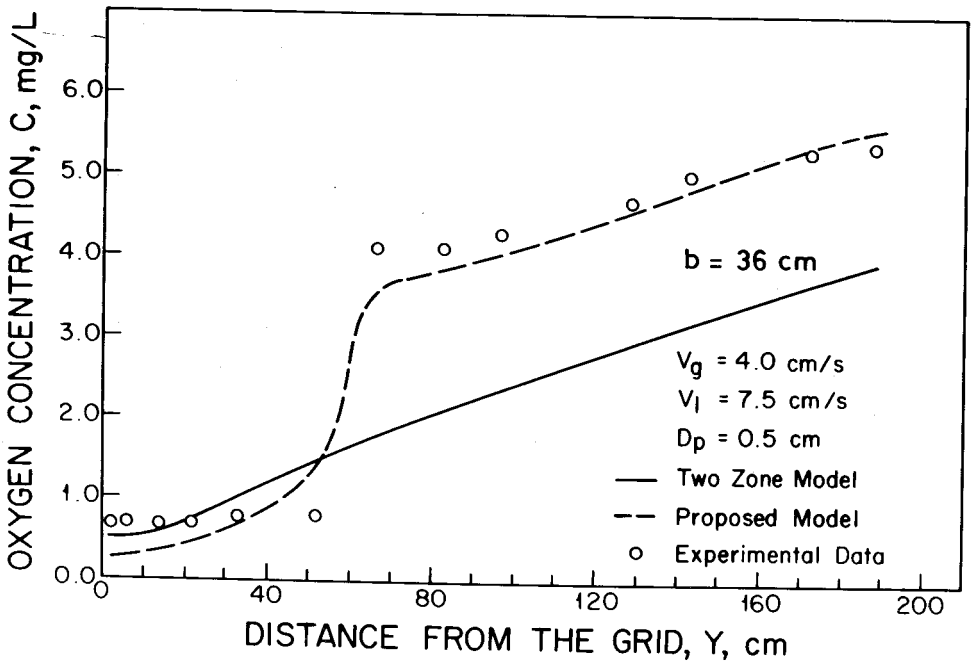

Figure 8 : Experimental and Predicted Oxygen Concentrations. Experimental Data were Reported by Alvarez-Cuenca, (1979).

Alvarez-Cuenca (1979) reported the same trend at low gas superficial velocities. The concentration was essentially constant up to 50 cm above the distributor. However, in this study the concentration remained constant up to 24 cm above the grid. This disagreement may be attributed to difference in the solid phase concentrations used in both studies. Alvarez-Cuenca (1979) reported using about 13 kg of solids whereas about 6 kg of solids have been employed in this study. Note that the columns used in both studies had the same volume.

3.2 Testing the Validity of the Proposed Model and its Comparison with the Two-Zone Model.

As indicated earlier, the proposed model is characterized by three pararmeters; viz. $(K_La)_B$, and E_y in the bulk zone. Consequently, it is not surprising that the proposed model fits the experimental data better than any existing model under the conditions of this study.

It may be argued that the proposed model conforms more closely to the experimental data since it contains more adjustable parameters than the other models. That could be partly true; but, in the present author's opinion, it mainly fits the data better than other models because it recognizes the different regions of mass transfer in a more realistic fashion than the existing models.

Figures 7 to 10 clearly indicate that the proposed model conforms more closely to the experimental data than the two-zone model.

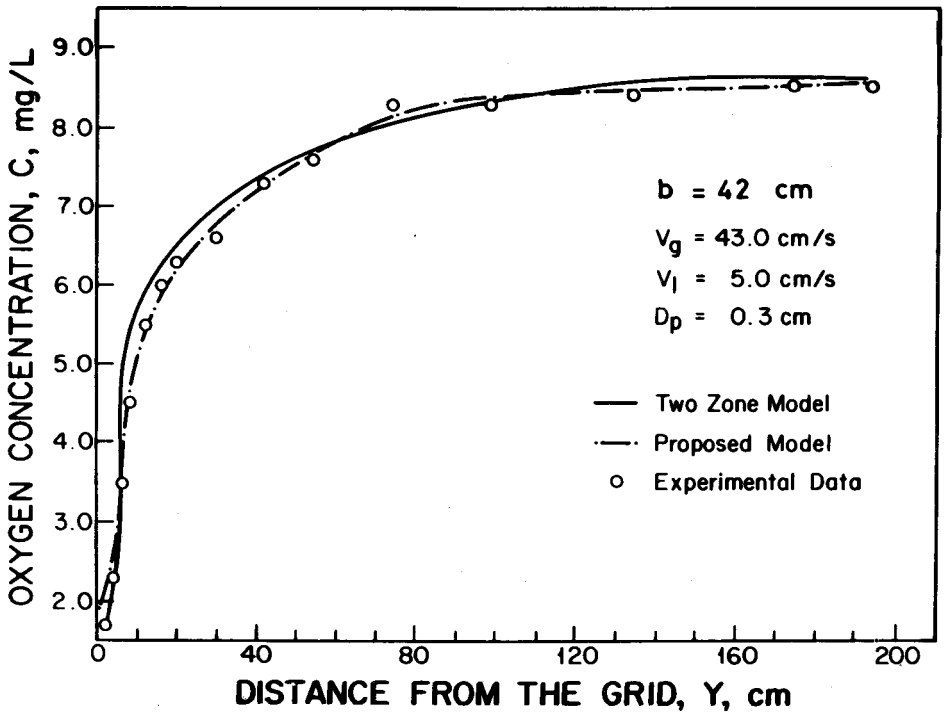

Figure 9 : Experimental and Predicted Oxygen Concentrations.

Some of the experimental data reported by Alvarez-Cuenca (1979) were utilized in Figure 8 to compare the experimental concentration profiles with those profiles predicted by both the two-zone model and the proposed model at low gas and liquid superficial velocities. It is clear from that figure that the proposed model provides a better description of the concentration profile than the T-ZM under such conditions.

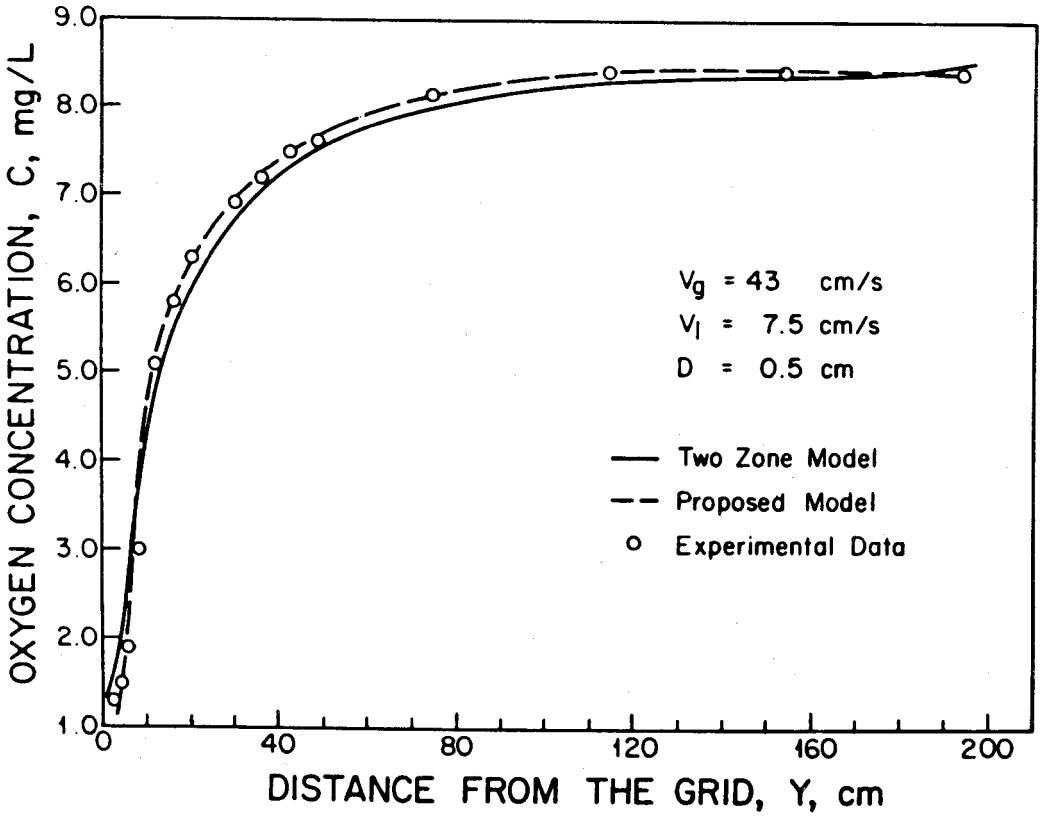

Figure 10 : Experimental and Predicted Concentrations.

Tables 1 and 2 show a direct correspondence between the gas superficial velocity and $(K_La)_G$ in three-phase fluidized beds. This is generally attributed to the increased formation of bubbles with gas flow rate, hence enhancing turbulence, which results in lhigher volumetric mass transfer coefficient in the grid zone evaluated by the proposed model increases with the liquid superficial velocity.

Table 1 : Volumetric Mass Transfer Coefficients $(K_La)_G$ Evaluated by the Proposed Model. Solid Phase Particle Diameter = 0.3 cm.

V_g \ V_L	5.0	7.5	12.0
8.0	0.073 (0.013)	0.105 (0.031)	0.182 (0.058)
26.0	0.238 (0.022)	0.322 (0.040)	0.424 (0.063)
43.0	0.342 (0.018)	0.475 (0.032)	0.490 (0.050)

$(K_La)_B$ in parenthesis.

Table 2 : Volumetric Mass Transfer Coefficients $(K_La)_G$ Evaluated by the Proposed Model. Solid Phase Particle Diameter = 0.5 cm.

V_g \ V_L	5.0	7.5	12.0
8.0	0.065 (0.028)	0.140 (0.046)	0.292 (0.065)
26.0	0.168 (0.016)	0.291 (0.055)	0.421 (0.059)
43.0	0.228 (0.041)	0.345 (0.049)	0.525 (0.057)

$(K_La)_B$ in parenthesis.

The results in Tables 3 and 4 suggest that, in the three-phase fluidized beds mode of operation the axial dispersion coefficient in the bulk zone is not a strong function of gas superficial velocity. However, it seems that the values of axial dispersion coefficient in the bulk zone are strongly influenced by the liquid superficial velocity.

Table 4 : Axial Dispersion Coefficients in the Bulk Zone.
Solid Phase Particle Diameter = 0.5 cm.

V_g \ V_L	5.0	7.5	12.0
8.0	4.21	4.80	4.90
26.0	2.41	4.30	5.00
43.0	2.64	3.56	4.00

Table 3 : Axial Dispersion Coefficients in the Bulk Zone.
Solid Phase Particle Diameter = 0.3 cm.

V_g \ V_L	5.0	7.5	12.0
8.0	4.67	5.36	6.39
26.0	2.12	2.61	4.19
43.0	2.20	3.60	4.17

4. CONCLUSIONS

The most relevant findings of this investigation can be summarized as follows:

(i) The existence of two distinct mass transfer zones in three-phase fluidized beds contradicts the application of one model, e.g. the plug flow or the axial dispersion model to describe mass transfer in such situations.
(ii) The proposed model conforms more closely to experimental data than the two-zone model under all the operating conditions employed in this study.

Nomenclature

b	Separation boundary parameter, cm
C_o	Dissolved oxygen concentration at the column entrance, mg/L
C	Dissolved oxygen concentration, mg/L
C_1	Dissolved oxygen concentration in the grid zone, mg/L
C_2	Dissolved oxygen concentration in the bulk zone, mg/L
C*	Dissolved oxygen equilibrum concentration, mg/L
C	= C* − C, mg/L
E_y	Axial dispersion coefficient, cm^2/s
K_La	Volumetric mass transfer coefficient, s^{-1}
K_1, K_2	Constant in eq. (A.11)
L	Column height, cm
M	Parameter defined by eq. (A.4)
V	Superficial velocity, cm/s

Greek Letters

θ	Parameter defined by eq. (A.8)
μ	Parameter defined by eq. (A.9)
Φ	Partameter defined by eq. (A.10)

Subscripts

B	Bulk zone
G	Grid zone
g	Gas
L	Liquid

5. REFERENCES

1. **Alvarez-Cuenca, M.,** Ph.D. Thesis. The University of Western Ontario, London, Ontario, Canada (1979).

2. **Alvarez-Cuenca, M., Nerenberg, M., Baker,** C.G.J. and **Bergougnou** M. "Mass Transfer Models for Bubble Columns and Three-Phase Fluidized Beds", 29th Canadian Chemical Engineering Conference, Sarnia, Ontario (1979).

3. **Alvarez-Cuenca, M., Nerenberg, M.** and **Asfour, Abdul- Fattah, A.** "Mass Transfer Effects Near the Distibutor of Three-Phase Fluidized Beds", I & EC Fundamentals, Vol. 23, 1984, pp. 381-6.

4. **Cherry, R.S., Sharonard,** A.C. and **Chen, Z.P.** "Parameters Influencing Dispersion in Three-Phase Fluidized Beds", Report ORNL/MIT. (1978), 254 pages.

5. **Deckwer, W.D., Buchkart, R.** and **Zoll, G.** "Mixing and Mass Transfer in Tall Bubble Columns", Chem. Eng. Sci., Vol. 29 (1974), pp. 2177-2188.

6. **Deckwer, W.D., Nguyen-Tien, K., Kelkar, B.G.** and **Shah.Y.T.** "Applicability of Axial Dispersion Model to Analyze Mass Transfer Measurements in Bubble Columns", AIChE J., Vol. 29 (1983), pp. 915-921.

7. **Dhanuka, V.R.** and **Stepanek, J.B.** "Gas Liquid Mass Transfer in Three-Phase Fluidized Beds, in Fluidization, ed. J.R. Grace and J.M. Matsen, Plenum Press, New York, pp. 261-269, (1980).

8. **Lee, J.C.** and **Worthington, H.** "Gas-Liquid Mass Transfer in Three-Phase Fluidized Beds, Instn. Chem. Engrs. Symp. Ser. No. 38, Paper B2, London (1986).

9. **Nhaesi, A.H.,** M.A.Sc. Thesis, University of Windsor, Windsor, Ontario, Canada, (1986).

10. **Ostergaard, K.** and **Suchozerbrski, W.** "Gas-Liquid Mass Transfer in Gas-Liquid Fluidized Beds", Proc. 4th European Symp. Chem. Reactor Eng., pp. 21, Pergamon Press, Oxford, (1971).

11. **Ostergaard, K.** and **Fosbol, P.** "Transfer of Oxygen Across the Gas-Liquid Interface in Gas-Liquid Fluidized Beds", Chem. Eng. J., Vol. 3, (1972), pp. 105-112.

APPENDIX A

Development of the Proposed Model

The approach adopted in the development of this model involves interfacing of a PFM and an ADM at the boundary between the grid and bulk regions. The proposed model contains three parameters; viz. the volumetric mass transfer coefficient in the grid zone. $(K_L a)_G$, and the axial dispersion coefficient in the bulk zone, E_y. The mathematical derivation is given given below.

Grid Zone

The differential equation and the corresponding boundary conditions are:

$$\frac{dC_1}{dy} = \frac{(K_L a)_G}{V_L} (C^* - C_1) \quad 0 < y < b \tag{A.1}$$

Boundary condition :

$$C_1 = C_o \quad \text{at} \quad y = 0 \tag{A.2}$$

The solution of Equation (1) is :

$$C_1 = C^* - (C^* - C_o)\, e^{-My} \tag{A.3}$$

where

$$M = \frac{(K_L a)_G}{V_L} \tag{A.4}$$

Bulk Zone

The mass balance equation is given by :

$$E_y \frac{d^2 C_2}{dy^2} - V_L \frac{dC_2}{dy} + (K_L a)_B (C^* - C_2) = 0 \tag{A.5}$$

If one considers :

$$C^* - C_2 = C_2$$

then

$$E_y \frac{d^2 C_2}{dy^2} - V_L \frac{dC_2}{dy} + (K_L a)_B \; C_2 = 0 \qquad \text{(A.6)}$$

The solution of Equation (6) is given by :

$$C_2 = K_1 \; e^{\theta y} + K_2 \; e^{\mu y} \qquad \text{(A.7)}$$

where

$$\theta = \frac{V_L}{2E_y} (1 + \Phi) \qquad \text{(A.8)}$$

$$\mu = \frac{V_L}{2E_y} (1 - \Phi) \qquad \text{(A.9)}$$

$$\Phi = \left[1 + \frac{4E_y \; (K_L a)_B}{V_L^2} \right]^{1/2} \qquad \text{(A.10)}$$

Equation (7) can be rewritten as follows :

$$C_2 = C^* - K_1 \; e^{\theta y} - K_2 \; e^{\mu y} \qquad \text{(A.11)}$$

Realising that :

$$\frac{dC_2}{dy} = 0 \quad \text{at} \quad y = L \qquad \text{(A.12)}$$

and that the flux continuity equation is given by :

$$V_L\ C_1\ (b-)\ =\ -E_y \frac{dC_2}{dy}\ (b+) + V_L\ C_2\ (b+)\ \text{at}\ y = b \qquad \text{(A.13)}$$

PFM ADM

Then using Equations (11), (12) and (13), one can obtain :

$$K_1 = \frac{-(C^* - C_o)\ V_L\ e^{-Mb}\ \ \mu/\theta}{\mu E_y (e^{\theta b} - e^{[(\theta-\mu)L+\mu b]}) - V_L([\mu/\theta]e^{\theta b} - e^{[(\theta-\mu)L+\mu b]})} \qquad \text{(A.14)}$$

$$K_2 = \frac{(C^* - C_o)\ V_L\ e^{[-Mb+\ (\theta-\mu)L]}}{\mu E_y (e^{\theta b} - e^{[(\theta-\mu)L+\mu b]}) - V_L([\mu/\theta]e^{\theta b} - e^{[(\theta-\mu)L+\mu b]})} \qquad \text{(A.15)}$$